Measurement and Simulation of Field Homogenity Inside Semi-anechoic Chamber

M. Bittera, J. Hallon, V. Smieško

Department of Measurement, Faculty of Electrical Engineering and Information Technology, Bratislava, Slovakia
Email: bittera@elf.stuba.sk

Abstract. *Nowadays in EMC area shielded rooms especially semi-anechoic chambers are used for EMI testing more often than open area test sites. To determine how the semianechoic chambers replace free-space test sites an unusual method of field homogenity determination by using field mapping measurements as well as simulations is described in this paper. The obtained results are compared with theoretical requirements.*

Keywords: semi-anechoic chambers, field homogenity, field mapping, finite-element method

1 Introduction

Using of interior shielded test sites (both anechoic and semi-anechoic) for EMC measurements have become more and more popular during the past years. It is because there are some noticeable advantages of the shielded room over classical Open Area Test Site (OATS) like stable background noise and immunity to weather conditions. However, when the shielded room replaces the OATS test environment, reflections from the walls of the shielded enclosure must be sufficiently suppressed for whole measured frequency range (from 30 MHz to 1000 MHz).

The quality of these semi-anechoic chambers (SAC) can be evaluated in a number of different ways. For example for radiated emission testing, we can use the general approach to measure the Normalised Site Attenuation according to international standards [1,2]. However, this test covers only a limited part of the chamber so obtained results from measurements do not characterise the field homogenity inside whole analysed chamber. Hence, we must apply other method to obtain information about chamber behaviour, e.g. presence of undesired resonance. One of possible methods is field mapping inside the analysed chamber over a whole frequency range. Unlike measurement published in [3] the vertical plane of antenna movement was chosen for this mapping. Theoretical values are compared with those ones obtained by measurement as well as simulations.

2 Theoretical analysis

While interpreting electric fields within ideal test site we consider a transmitting antenna with a gain *G*. The antenna is fed by a matched source and the radiated power P_T. The free-space far-zone field strength *E* at a distance *d* is given [4] :

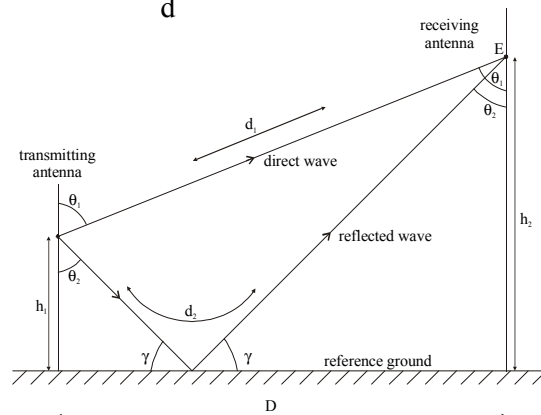$$E = \frac{\sqrt{30P_T G}}{d} e^{-j\beta d} \qquad (1)$$

Fig. 1 Elm waves transmission over conductive floor

where β is the phase constant. In the case of radiated emission test sites only the equivalent value of field strength in the place of receiving antenna is interesting. It is given by the direct wave as well as ground plane reflected wave as it is shown in Fig. 1. So for horizontally polarised antennas Eq. 1 becomes generally :

$$E_H = \sqrt{30 P_T G}\left(\frac{e^{-j\beta d_1}}{d_1} + \rho_H \frac{e^{-j\beta d_2}}{d_2}\right) \quad (2)$$

where ρ_H is the reflection coefficient and d_1, d_2 are path lengths of direct and reflected waves. Likewise for vertically polarised small dipoles Eq. 1 becomes :

$$E_V = \sqrt{30 P_T G}\left(\frac{e^{-j\beta d_1}}{d_1}\sin^2\theta_1 + \right.$$
$$\left. + \rho_V \frac{e^{-j\beta d_2}}{d_2}\sin^2\theta_2\right) \quad (3)$$

where angles θ_1 and θ_2 are evident from Fig.1. However, Eq. 2 in comparison with Eq. 3 is suitable only if receiving dipole is situated in the same axis as transmitting one in the distance D. If receiving dipole is deflected from this axis Eq. 2 is changed to the form :

$$E_H = \sqrt{30 P_T G}\left(\frac{k_1^2 e^{-j\beta d_1}}{d_1} + \rho_H \frac{k_2^2 e^{-j\beta d_2}}{d_2}\right) \quad (4)$$

where k_i is the correction factor of receiving antenna deflection, which includes also the direction patterns of used antennas. In our case small dipoles are used so the correction factor k_i is given by the following formula :

$$k_i^2 = \frac{h_i^2}{h_i^2 + D^2} + \frac{D^2}{h_i^2 + D^2} \cdot \frac{D^2}{w^2 + D^2} \quad (5)$$

and h_i is the difference between heights of receiving dipole h_2 and transmitting dipole h_1 or their sum. It depends on the fact whether direct or reflected electromagnetic wave is assumed, w is deflection of receiving antenna from axis. Using Eq. 3 and 4 we are able to calculate the field strength values at points of the mapping plane. Calculated field distribution for horizontally polarised dipoles is in Fig. 3.

3   Measurement

The field mapping technique is very useful method to evaluate general chamber quality. On the other hand this class of measurements is very time consuming especially for larger chamber. The field mapping was realised using receiving dipole which was moved over mapping plane in order to obtain chamber properties useful for radiated emission measurements like undesired resonance or strange devices influence to field distribution inside the chamber.

A block diagram of the measuring system is shown in Fig. 2. The measurement was realised in semi-anechoic chamber of Laboratory of electromagnetic compatibility FEI STU in Bratislava (LEMC). A half-wavelength dipole placed in a chamber's axis at a one-meter height from the metal floor was used as a source. As a receiver antenna short dipole was used to reduce its own influence to measuring value. Cables and other important components for measurement were situated according to relevant international standard for field measurement [1]. Receiving dipole was moved and the field strength was measured over the whole mapping area on 0.1 by 0.1 meters grid. Every measurements was repeated five times to improve measurement uncertainty [5].
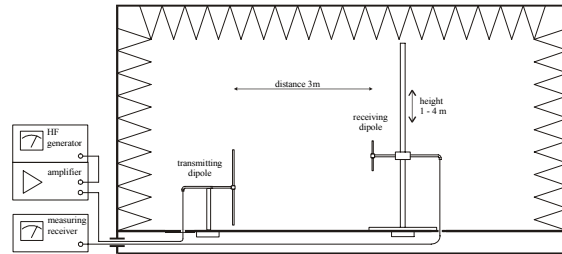

Fig. 2 Field mapping measuring system

Measurements were realised for both horizontal and vertical polarisation over the whole frequency range. Fig. 4 and 6 shows an example of field distribution at frequency 50MHz on our mapping plane.

4   Simulations

The other ways to obtain information about chamber properties are simulations. The Finite Element Method (FEM) was chosen from plenty of numerical methods. It is, because FEM offers easy way of modelling inhomogeneous structures and therefore it is suitable to simulate as complex object as semi-anechoic chamber [6]. FEM is used for modelling problems by breaking down the computational domain into a set of simple subdomains called finite elements. Then, the variational approach is applied over each finite element. Thus, as geometry of the elements is simple, it is possible to systematically construct the basis and the test functions needs for variational approach. A set of discrete integral equations is obtained for each finite element and they

are assembled all together in a global system of equations that, after the imposition of the boundary conditions, characterise the behavior of the system under analysis. Once the system of equation is solved the solution is obtained. Usually the intensities of electric fields are calculated at the edges of each tetrahedron using variational methods and by means of them we can obtain other field quantities in whole solution domain using miscellaneous post-processes.

Dimensions $4.5m \times 8.5m \times 4.5m$ of test site's model are given by dimensions of real chamber of LEMC. This semi-anechoic chamber has infinitely conductive floor and its walls and ceiling are embosomed with ferrite tile absorbers. Ferrite tile absorbers represent the 6.3mm thick layer with material constants (relative permittivity/permeability and conductivity) of F42 material [7] for given frequency. Also half-wavelength dipole antenna is used as a radiator and field strength E is scanned over the given mapping plane 3m separated from transmitting dipole. Simulation result for horizontally polarised dipoles is shown in Fig. 5.

5 Results

Results from theoretical calculation, measurement and also simulations are shown in Fig. 3-8 (calculated and simulated fields for vertical polarisation are missing for the sake of limited range of the article). Despite of theoretical results, which are valid for ideal free-space test sites, other ones are obtained for semi-anechoic chamber. The measurements within chamber are influenced by interferences of undesired reflection from absorbing material. These facts cause maximal error ±1.6dB between calculated and measured field values for horizontally polarised dipoles and ±3.6dB for vertical polarisation. (see Fig. 7 and 8). Greater error at vertical polarisation is caused in addition to occurred reflections also by geometry of additional devices e.g. cables, antenna mounts, which are oriented parallel to measuring antennas and therefore increase the error of measurement. Another indication of tested site obtained from measurement is asymmetry of field distribution. Measured asymmetry (±1dB for both horizontal and vertical polarisation) may be caused by imperfections of analysed chamber. Similar results are obtained using simulations using

FEM. As we can see the field distribution is not symmetrical too, which is caused by unequal division of analysed space by FEM.

6 Conclusions

An unusual method of field homogenity determination within semi-anechoic chamber is described in this paper. In spite of time consumption that is necessary for field mapping measured results give us realer vision about the performance of absorbers across the entire chamber than do traditional certification tests. If the simulated data are validated through the measurement, simulations would replace the rest of the measurements and it leads to time saving.

References
 [1] CISPR 16-1: Radio disturbance and immunity measuring apparatus. IEC international standard, 1993.
[2] EN 50147-2 Anechoic Chambers, Part 2: Alternative test site suitability with respect to site attenuation. European Standard.
[3] Smith, A.A., German, R.F., Pate, J.B.: Calculations of site attenuation from antenna factors. IEEE Transactions on EMC, Vol.24, 1982, pp.301-316.
[4] Archambeault, B., Holloway, C.L., McKenna, P.: Measurements and simulations of a semi-anechoic room using field mapping. IEEE 2002 International Symposium on EMC, Austin 2002, pp. 947-951.
[5] Heise, E.R., Heise, E.R.W.: A method to calculate uncertainty of radiated measurements. IEEE 1997 International Symposium on EMC, Austin 1997, pp.359-364.
[6] Bittera, M., Kováč, K., Smieško, V.: FEM modelling for field predictions inside semi-anechoic chambers. Journal of Electrical Engineering, No.9/s, Vol.53, 2002, pp.174-177.
[7] Smieško, V., Kováč, K. Harťanský, R., Hallon, J.: Use of the cascade matrix technique in determination of the performance of multi-layer absorbing structures based on ferrite tiles. 14-th International Wroclaw Symposium and Exhibition on Electromagnetic Compatibility, Wroclaw 1998, pp. 400-404.
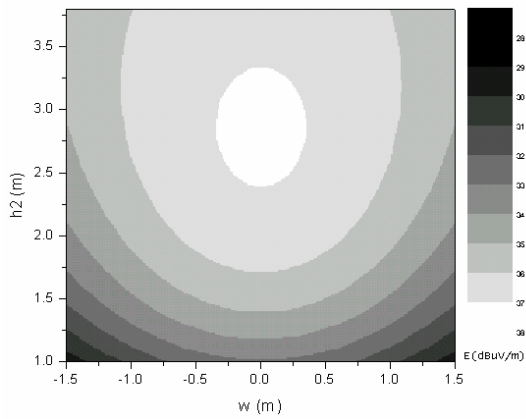
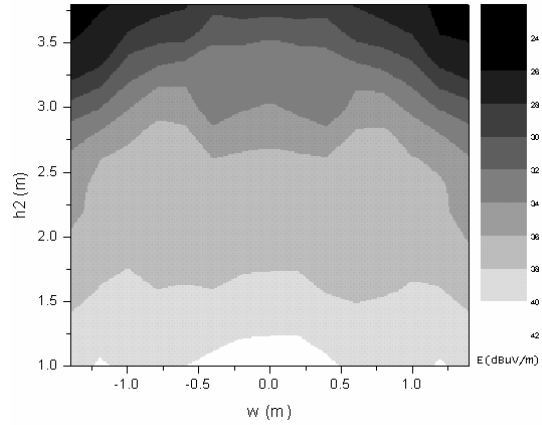Fig. 3 Calculated field distribution for horizontally polarised dipoles at 50MHz

Fig. 6 Measured field distribution for vertically polarised dipoles at 50MHz
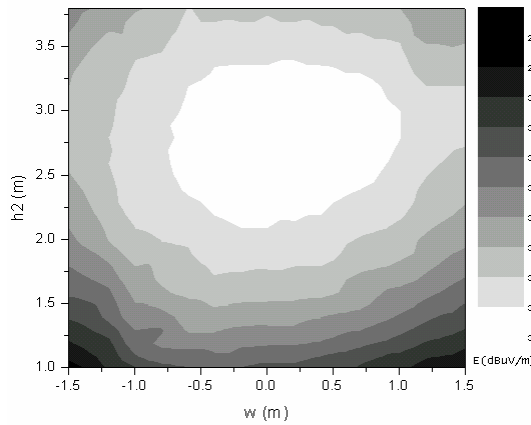

Fig. 4 Measured field distribution for horizontally polarised dipoles at 50MHz
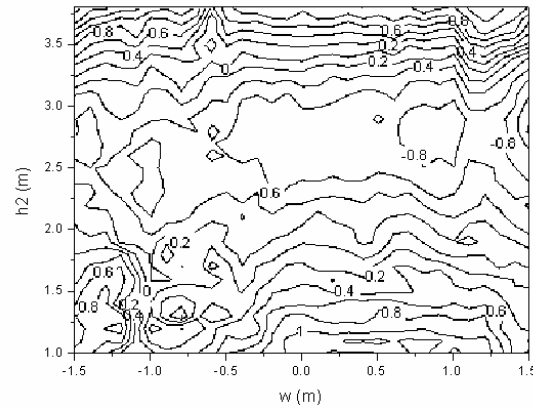

Fig. 7 Difference between measured and calculated field distribution for horizontally polarised dipoles at 50MHz (in dB)
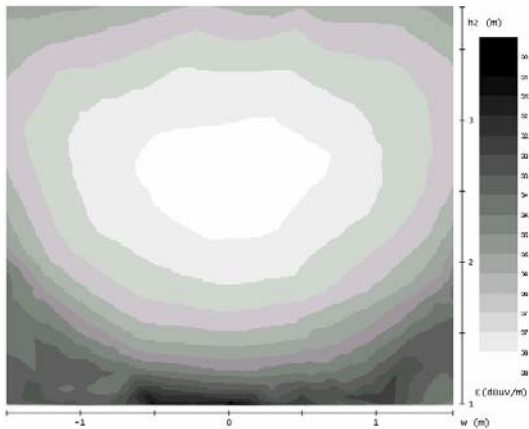

Fig. 5 Simulated field distribution for horizontally polarised dipoles at 50MHz
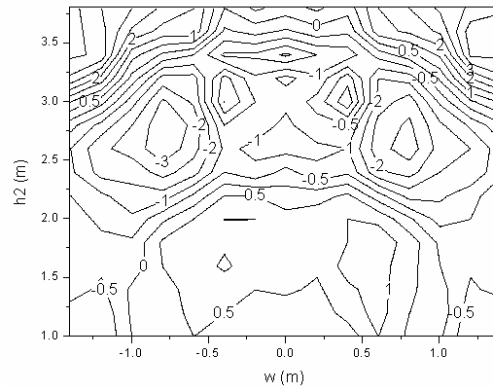

Fig. 8 Difference between measured and calculated field distribution for vertically polarised dipoles at 50MHz (in dB)